Space Shuttle Testing of the TriDAR 3D Rendezvous and Docking Sensor

Stéphane Ruel, Tim Luu, and Andrew Berube
Neptec Design Group, 302 Legget Drive, Kanata, Ontario K2K 1Y5, Canada
e-mail: sruel@neptec.com, tluu@neptec.com, aberube@neptec.com

Received 6 January 2011; accepted 26 August 2011

This paper presents results from the first two Space Shuttle test flights of the TriDAR vision system. TriDAR was developed as a proximity operations sensor for autonomous rendezvous and docking (AR&D) missions to noncooperative targets in space. The system does not require the use of cooperative markers, such as retroreflectors, on the target spacecraft. TriDAR includes a hybrid three-dimensional (3D) sensor along with embedded model based tracking algorithms to provide six-degree-of-freedom (6 DOF) relative pose information in real time. A thermal imager is also included to provide range and bearing information for far-range rendezvous operations. In partnership with the Canadian Space Agency (CSA) and NASA, Neptec has space-qualified the TriDAR vision system and integrated it on board Space Shuttle Discovery to fly as a detailed test objective (DTO) on the STS-128 and STS-131 missions to the International Space Station (ISS). The objective of the TriDAR DTO missions was to demonstrate the system's ability to perform acquisition and tracking of a known target in space autonomously and provide real-time relative navigation cues. Knowledge (reference 3D model) about the target can be obtained on the ground or in orbit. Autonomous operations involved automatic acquisition of the ISS and real-time tracking, as well as detection and recovery from system malfunctions and/or loss of tracking.

1. INTRODUCTION

In 2010 the United States government unveiled a new direction for its space program via the NASA Authorization act of 2010. As part of this plan, autonomous rendezvous and docking (AR&D) was identified as a key enabling technology. This technology is required not only for future space exploration initiatives but also to develop the ability to extend the life of valuable assets in orbit via in-orbit servicing. AR&D with cooperative targets has been demonstrated in space. The Russian Progress and Soyuz, as well as the Japanese HTV and European ATV, are vehicles capable of automatically docking with the International Space Station (ISS) (ESA, 2008; ESA Media Relations Office, 2008; Fehse, 2003). NASDA (now JAXA) and DARPA also tested rendezvous and docking and other satellite-servicing technologies in space in the ETS-VII and Orbital Express programs (Howard et al., 2008; Mokuno, Kawano, & Kasai, 1999; Mokuno, Kawano & Suzuki, 2004). Missions performed to date operate on the assumption of a controlled, cooperative target. Furthermore, onboard sensors on the chaser spacecraft relied on reference targets, typically retro reflectors, positioned on the target vehicle.

Unfortunately, many of the important scenarios that would require AR&D technology involve elements that were not or could not be planned during mission design. A spacecraft in need of servicing may not have been designed to be captured and would not include the necessary hardware, such as target markers or docking ports. Even if it had reference markers, failure modes (such as lack of fuel) might prevent the chaser vehicle from properly tracking the target. Under these constraints, the chaser spacecraft would be required to have the ability to rendezvous with a target that was noncooperative and potentially tumbling.

Neptec's TriDAR vision system was developed to serve as a guidance sensor for AR&D operations in proximity to noncooperative targets. The system was designed to provide six-degree-of-freedom (6 DOF) relative pose in real time without requiring specific markers on the target spacecraft. To achieve this, the system uses a laser-based three-dimensional (3D) sensor. TriDAR's onboard software uses geometric information contained in successive 3D point clouds to match against the known shape of the target object and calculate its position and orientation. Knowledge about the shape of the target can be obtained on the ground (via CAD model or scan data) or from data acquired in orbit if the target was unknown before launch (Creamer, 2007). The computer vision algorithms developed by Neptec allow this process to be performed in real time on TriDAR's embedded flight computer, although achieving the robustness and reliability necessary for mission critical operations (Ruel, English, Anctil, & Church, 2005). TriDAR also includes a thermal imager used to provide bearing and range information at ranges exceeding that of the active 3D sensor.

Multimedia files may be found in the online version of this article.

TriDAR was originally developed for an automated servicing mission to a noncooperative target: NASA's Hubble Robotic Vehicle (HRV) mission. After the Columbia tragedy, the Space Shuttle could only fly to the ISS, which could serve as a safe haven in the event that the vehicle was damaged during ascent. The HRV was meant as an automated vehicle that would use the TriDAR to rendezvous with, capture, and robotically service the Hubble Space Telescope (HST). The mission was later cancelled, as the Space Shuttle was ultimately cleared to perform the HST servicing mission (STS-125), but TriDAR development continued. The capabilities of the TriDAR prototype that resulted from this effort were later demonstrated at various test facilities, including NASA's Marshall (MSFC) and Goddard Space Flight Centers (GSFC), the Naval Research Laboratory (NRL), and the Canadian Space Agency (CSA) (Creamer, 2007). Following successful testing of the technology, NASA and CSA selected the TriDAR as a detailed test objective (DTO) on board Space Shuttle Discovery for the STS-128 and STS-131 missions.

This paper introduces the TriDAR relative navigation vision system and presents results from the system's first two test flights on board the Space Shuttle. Section 2 presents the challenges associated with developing AR&D sensors for space using computer vision. Section 3 details the approach developed for the TriDAR tracking system. Section 4 presents the hardware developed to implement the tracking system. Section 5 presents results from the first two test flight of TriDAR technology on board the Space Shuttle.

2. VISION SYSTEMS FOR NONCOOPERATIVE AUTONOMOUS RENDEZVOUS AND DOCKING

This section introduces the unique characteristics and challenges associated with vision system design for AR&D in space. This section will serve as a reference to explain the design approaches presented in the following sections.

2.1. The Rendezvous and Docking Process

Rendezvous and docking in space involve a passive vehicle, referred to as the target, and an active vehicle, referred to as the chaser. Rendezvous missions typically involve five major phases: launch/orbit insertion, phasing, far range rendezvous, close range rendezvous, and mating/berthing (Fehse, 2003). The first two phases rely on absolute navigation measurements such as GPS or ground radar. Relative measurements using sensors on board the chaser are typically required within a few kilometers (∼5 km) of the target during the far rendezvous phase. At this point, relative measurements of range and direction (by radar, LIDAR, or other means) or relative position (e.g., GPS or RGPS), along with relative rates, are used to plan maneuvers necessary to approach the target for close range rendezvous. The final two phases of proximity operations will lead to vehicle mating conditions either via direct docking or via robotic capture (berthing). At this point, relative position, attitude, and rates between the two spacecraft must be obtained via direct or indirect measurements. This phase typically starts a few hundred meters away from the target, with the spacecraft entirely guided by its onboard sensors.

In cooperative target scenarios, it is often assumed that the target spacecraft is known and will hold a known attitude relative to the orbital plane and gravity vector. This assumption can be used to obtain indirect relative attitude measurements and alleviate the need to obtain relative attitude from the rendezvous optical sensor. Other strategies involve transmitting target attitude to the chaser to enable calculation of real-time relative attitude using inertial sensors. In noncooperative target scenarios, mission designers cannot assume that the target spacecraft will hold attitude or that it will be in a state where it can communicate with the chaser. In this case, the chaser must measure relative attitude directly to assess the location and relative motion of the docking port. In some servicing and military applications, it is also possible that the target is not known before the system is launched. These constraints drive a set of challenging additional requirements on the relative navigation sensor.

2.2. Vision Systems Design Challenges

Developing vision systems to operate in space is a challenging task. Systems involving precision optics and state-of-the-art components must survive very high launch loads, extreme temperatures, and radiation. The system must be reliable and rugged, although using little power and fitting in a compact, lightweight package. The observable scenes can also be extreme: from full sunlight to complete darkness (MacLean & Pinkney, 1993). For certain rendezvous scenarios, the earth could also be in the background, providing a nonstatic background scene, further complicating target segmentation. Processing platform and communications bandwidth constraints also severely limit the use of fast sensors (>10K samples/s) because of the large number of data generated in a short amount of time. Use of advanced vision processing algorithms is also difficult because of the limited processing resources available.

The characteristics of operations during the far and close rendezvous phases presented in the previous section lead to additional, AR&D specific design drivers:

Reliability: Perhaps the most obvious requirement is that the sensor must be sufficiently accurate and reliable to lead to a successful capture of the target.

Dynamic Range: The most challenging element comes from the combination of the required wide operating range, from several kilometers down to centimeters, and the nature of the target's surface. Spacecraft are typically covered

with white, dark, and/or reflective materials. The combination of these surface types can be highly problematic for passive or active optical sensors. A low-reflectivity target positioned at long range will produce a very weak signal, whereas a reflective target at close range could produce a signal millions of times stronger. Requirements for a wide sensor dynamic range constitute a fundamental design driver for AR&D vision sensors. The distances involved also cause problems to fixed-field-of-view sensors, for which the target size on the image plane will vary greatly with distance.

With the rendezvous sensor located on the chaser vehicle, the sensor will also be sensitive to attitude changes of the moving platform. A sudden attitude change of the chaser could result in a loss of tracking of the sensor. Fast automatic target acquisition is therefore a highly desirable feature, especially for missions involving limited human monitoring.

3. TRIDAR: THREE-DIMENSIONAL VISION-BASED GUIDANCE FOR NONCOOPERATIVE AUTONOMOUS RENDEZVOUS AND DOCKING

Neptec's TriDAR (triangulation + LIDAR) system results from over 7 years of research and development funded by the Canadian Space Agency (CSA) and NASA on multiple programs. TriDAR's algorithmic approach to tracking from 3D point cloud data was developed before the sensor was designed. Sensor hardware was then developed to best match the needs of the algorithmic approach and the application's specific AR&D requirements.

The concept at the source of TriDAR's algorithmic approach comes from research in automatic target recognition (ATR) from 3D LIDAR data performed at Neptec for Defense Research and Development Canada (DRDC) (English, Ruel, Melo, Church, & Maheux, 2004; Ruel et al., 2004). This research demonstrated that very little 3D information is necessary to extract high-level scene information such as finding ground, recognizing targets, or performing pose estimation. With sparse data covering the entire object or geometry of interest, it was shown that object recognition and pose estimation are possible with very similar success rates even if the source data are diminished by several orders of magnitude. In general, 100 3D measurement points was shown to be sufficient to achieve recognition and pose estimation of targets from a knowledge base of potential objects. Results also demonstrated that successful results can be achieved with articulated objects (e.g., turrets, doors) provided that the dominant geometric features of the object remain unchanged.

The AR&D application is a simpler case of the ATR problem, because target extraction from a cluttered scene (segmentation) is not necessary in space and tracking is limited to a single instance of a known object. ATR research demonstrated that pose estimation and tracking should be possible without requiring a large number of 3D data, provided that they are well distributed over the target. Therefore, only a small number of 3D measurements need to be collected, transferred, and processed, making real-time operations possible on flight processor hardware. This led to the development of the more information, less data (MILD) approach used by the TriDAR AR&D sensor, in which the system tries to extract maximum geometric information at minimal cost in terms of processing and data volume (English, Okouneva, Saint-Cyr, Choudhuri, & Luu, 2011). Using this strategy, only sparse data that will be directly used to perform the pose estimation (typically ~1,000 3D measurements) are acquired by the sensor (Ruel et al., 2006). As shown during ATR research, as few as 100 3D samples can be sufficient for successful operations, but more points can be used, depending on the available sensor, processing resources, and target geometry. The data can be acquired over an area of interest on the target object (if its current position is known) or over the entire field of view of the sensor if nothing is known of the target position, as in the early stages of tracking acquisition.

This approach is fundamentally different from typical target-based solutions, which need to acquire a large number of data to locate points of interest such as retro-reflectors on the target. These points are also typically relatively close to each other for practical reasons, limiting their use to measure relative attitude (Polites, 1998). Once the reference points are located (typically fewer than five), only these 3D coordinates are directly used in computing the relative pose. In the approach developed for TriDAR, the sensor sparsely samples the target surface over a large area and directly matches all the acquired 3D data against the reference model of the object. The object effectively becomes the target and all the data acquired can be used directly in computing the relative pose. This is the equivalent of using hundreds of retro-reflector targets covering a large area over the target geometry. This strategy results in better sensor noise averaging and more stable and accurate relative pose measurement. The obvious limitation is that the reference model needs to be of sufficient resolution and accuracy for the desired system performance and sensor noise characteristics. Models with lesser fidelity can still be used, but the performance of the system will degrade accordingly.

3.1. Target Acquisition and Tracking Initialization from Three-Dimensional Point Cloud Data

The pose estimation algorithm used for tracking (see next section) is a minimization process requiring an initial guess. Once tracking is established, the initial guess comes from the last known position or predictions from internal filters, depending on the operation. A different algorithm is therefore necessary to initialize the system or recover from loss of tracking. TriDAR can accept external inputs to seed the algorithm, either from other sensors or from the ground, or use its internal algorithm. One such algorithm is the polygonal aspect hashing (PAH) technique developed at Neptec

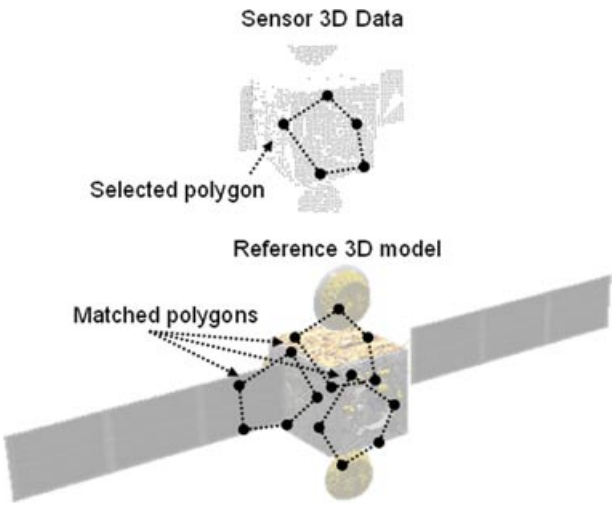

Figure 1. Search space reduction by polygon matching.

(Ruel, Luu, Anctil, & Gagnon, 2008; Ruel, Ouellet, Luu, & Laurendeau, 2008). Although detailed information about this algorithm has not been approved for release, this section presents an overview of its operating principles.

The PAH algorithm follows the same smart sensing or MILD strategy used for the tracking algorithm and only acquires data that will be used to extract the desired high-level geometric information from the scene (English et al., 2011). The PAH algorithm does not require organized data such as a raster grid. Therefore, various fast scan patterns can be used to generate the sparse data required. This minimizes data acquisition and transfer time. PAH was designed to be robust to occlusions and various artifacts found in active sensor data, such as distortions caused by laser beam divergence and specular reflections. The algorithm is able to find its target on flight processing hardware in typically 5–10 s.

PAH requires an offline processing step where a reference database is generated from a 3D model of the target object. The run-time portion of the algorithm then uses that reference database to localize the target object efficiently in space relative to the sensor focal point. The technique uses a strategy where the data are aligned to a reference model in various poses until a best fit is obtained, much like a child trying to add a piece to a jigsaw puzzle (puzzle-fitting strategy). The difference in this case is that the pose search space has six dimensions. To avoid searching the entire six-dimensional space, the algorithm first reduces the search space to the set of poses that have some overlapping surfaces between the input scan data and the reference model. Poses that provide overlapping surfaces are found by matching polygons made from a few selected points from the input scan data to the model surface (Figure 1). Multiple polygons can be used to provide redundancy and increase the robustness to outliers. Once the search space has been reduced to the most likely candidates, the algorithm tests how well the data fit to the model surface for each identified pose.

3.1.1. Offline Processing

To optimize the run-time part of the localization, offline processing is needed to generate a lookup reference database. The database is composed of lookup hash tables that are used to efficiently perform the polygon-matching process. Let M be a polygonal model of the object to be localized and S a sparse set of 3D points s_i located on the model surface. The offline processing first generates the set of all segments $L(s_i, s_i)$ that can be created on M from point pairs of S. The set of segments is then arranged in hash tables that efficiently store length and connectivity information to allow direct segment lookup with linear complexity while keeping the database compact.

3.1.2. Runtime Localization

The runtime localization process uses the reference database created during the offline processing along with a sparse 3D point cloud obtained from a sensor to determine the position T and rotation R of the target model M with respect to the sensor focal origin C. The input point cloud I is composed of a set of n 3D points, p_i, defined with respect to C sampling the surface of M. The input point cloud is not expected to be organized in any specific pattern such as a grid. The point cloud can be sparse but should cover as much of the target as possible.

The first step of the algorithm is used to reduce the six dimensions pose search space. The search space is reduced by keeping the set of poses that have at least some overlapping surface between the input scan data and the reference model. To perform this, a polygon-matching process is used. First, an N-point polygon is selected from the input point cloud points p_i. Selection of N is a tradeoff between processing time for steps 1 and 2 and depends on the object's geometry. Typically, four- to six-point polygons are used. The points from the input data are selected to provide a polygon with a large surface area. This will provide more pose determination momentum and fewer polygon matches. Once a polygon is selected, the set of possible poses is reduced to the poses where the polygon input scan points $[p_i]_N$ line up with their corresponding model surface points $[s_i]_N$ within a specified tolerance. Finding all the matching polygons is done using the segment hash tables generated offline and is effectively a partial tree traversal process. The key to achieving maximum performance is to keep the reference model information sparse. This keeps the number of matches small although providing a good enough pose estimate for an iterative algorithm (e.g., iterative closest point (ICP)) to do the fine alignment.

For each polygon match, a set of N matched points $[p_i, s_i]_N$ is obtained. From each matched polygon pair, the

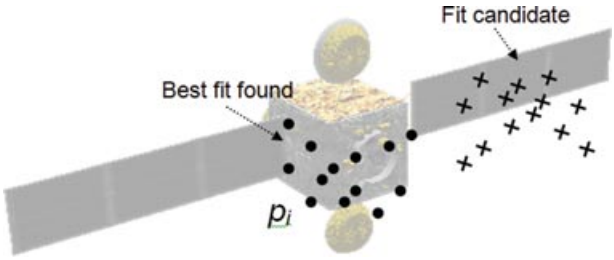

Figure 2. Surface fit check performed on pose candidates.

corresponding relative pose (T, R) can be computed. The points in each matched set are assumed to represent the same physical location on the object surface within the defined tolerance. Under this assumption, the two sets of matched points can be related by

$$[p_i]_N = R[s_i]_N + T, \tag{1}$$

where T is the 3×1 translation vector and R is the 3×3 rotation matrix representing the position and rotation of the target object with respect to the sensor focal point C. The rotation matrix, R, and translation vector, T, are then found via a pseudo-inverse computation. The pseudo-inverse can be easily calculated by singular value decomposition (SVD).

Once the set of pose candidates has been generated, the algorithm tests them to assess how well the point cloud points p_i line up with the surface of M (Figure 2), based on their distances. For each fit test, the p_i are transformed in the model reference frame using the rotation R and translation T calculated from the polygon-matching process. This surface alignment check has $O(n)$ complexity, where n is the number of points in the input point cloud. The pose candidate that aligns the point cloud best with the surface is selected as the winner. It is also possible to speed up the fit check process by performing a precheck step with a decimated (resolution reduced) dataset. The efficiency of this process depends on the number of points in the input point cloud.

After the best-fitting pose candidate has been determined, it is possible to repeat the process with more polygons from the same input point cloud or from newly acquired point clouds over time. Using either technique will increase the probability of success of the algorithm as well as increasing robustness to outliers. The approach to be used can be selected depending on operational considerations such as relative motion rates, processing time, and power available.

3.2. Tracking Algorithm Approach

The tracking algorithm operates by constantly acquiring sparse, unorganized 3D data from the target and performing a pose estimate for each point cloud acquired (Figure 3). Three-dimensional sensors provide information about the

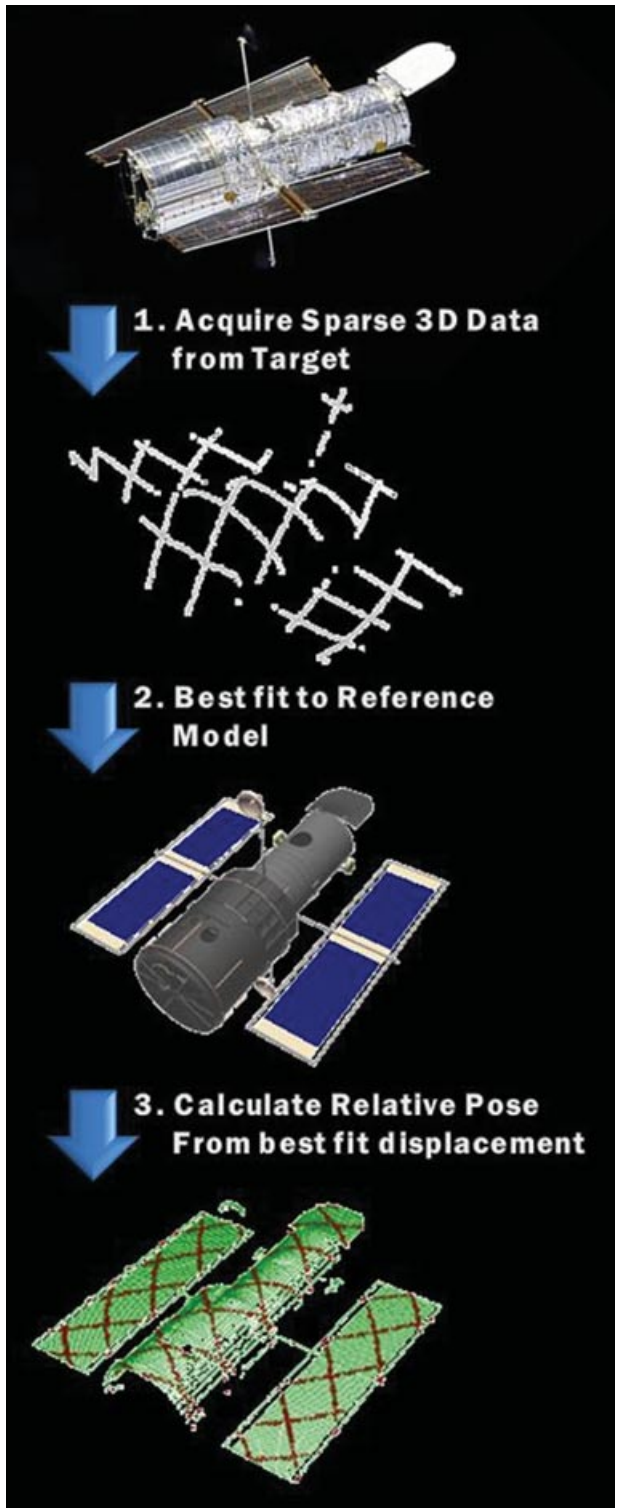

Figure 3. Tracking algorithm pose estimation process.

geometry of a scene directly. Therefore, there is no need to add reference markers on the target, because the target geometry provides a usable reference. The shape of the target is typically obtained from CAD models but could also be generated from sensor data acquired either in orbit or on the ground before flight (Ruel et al., 2005). In-orbit modeling of the target would be performed using fly-around maneuvers, during which the necessary data would be acquired (Obermark, Creamer, Kelm, Wagner, & Henshaw, 2007). The downlinked data would then be used to assemble the 3D model that would serve as a reference on the ground. The model resolution is selected based on the size of the features that will be tracked, operating ranges, sensor noise characteristics, and desired system performance. Typical model resolution is on the order of 1–5 cm. The resolution selected is also constrained by the available memory on board the processing platform.

To perform the pose estimation, the 3D data obtained are aligned to the reference model of the target using a proprietary variant of the ICP algorithm developed at Neptec and optimized for real-time operations. The ICP algorithm was simultaneously developed by Besl and Mackay (1992) and Chen and Medioni (1992). Many variants of the ICP approach have been proposed and tested to improve its speed or robustness (Rusinkiewicz & Levoy, 2001). The method developed by Neptec was tailored for real-time operations from unorganized sparse 3D data, although still providing good accuracy and stability. It was shown that pose accuracy on the order of 1 cm/1° can be achieved in real time (5 Hz) on a relatively small target (1 m) for final capture operations (<10 m). It was also shown that the performance of the algorithm is largely dependent on the target geometry (English et al., 2011). These results were achieved on a flight processor using 1024 3D measurements per frame (Ruel et al., 2005, 2006).

The ICP registration is an iterative minimization process that is initiated from an estimate of the relative pose. For space applications, objects move slowly enough so that the pose estimate from a previous tracking frame can be used as the initial guess. For faster moving objects, prediction filters can be used to predict the target location at the next frame. If no knowledge about target location is available, search algorithms such as the PAH presented in the previous section can be used.

Given an input 3D point cloud I composed of a set of n 3D points p_i defined with respect to the 3D sensor origin C and a reference surface model of the target M, the objective of the ICP is to find the rigid transformation (R, T) between I and M. This is accomplished by performing a best fit of the input point cloud data to the surface of M that requires minimizing

$$\min \sum_{i=1}^{n} [\text{dist}(Rp_i + T, s_i)]^2. \quad (2)$$

The ICP iterative process involves three main steps:

1. *Establish point correspondence:* Each 3D point p_i of the input point cloud I is matched to the closest surface point s_i of the reference model M, based on the current estimate of relative pose (R, T), where R is the rotation and T the translation. The matched coordinates are then assumed to correspond to the same physical location on the object. Outlier rejection can also be accomplished at this stage by rejecting matched points that are too far apart.
2. *Compute the transformation:* From the set of corresponding points (p_i, s_i), the relative transformation (R, T) that minimizes the sum of squared distances between the matched points can be computed. This is similar to the process described in Section 3.1.2.
3. *Apply the transformation:* The transformation (R, T) found in Step 2 is then applied to the input point cloud points p_i and the algorithm goes back to Step 1 unless a stop criterion is met. Typical stop criteria involve thresholds on specific performance metrics such as residual, number of iterations, or processing time.

The ICP algorithm has the advantage of having robustness characteristics that are needed for space operations (Besl & McKay, 1992). The ICP does not require preprocessing of the data, smoothing, or feature extraction and can operate directly on the input 3D points. The algorithm can also operate from occluded surfaces, provided enough distinct geometry is visible. ICP tolerates relatively high noise levels, on the order of 10% of the tracked feature size. On the other hand, the minimization process is sensitive to outliers, and proper outlier rejection methods must be used. The advantage of operating in space is that there is no scene clutter to segment, which simplifies the outlier rejection process.

3.3. Operational Modes

The TriDAR control software can operate in three different high-level states: bearing, search, and tracking. Figure 4 shows how the algorithm enters each operational mode.

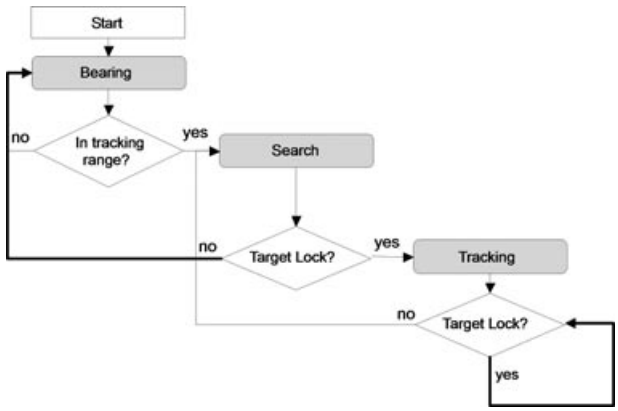

Figure 4. Operational modes logical flow.

Once initiated, the system enters the bearing mode. This mode only provides bearing, range, and closing rates of the target relative to the sensor. It is typically used during the far rendezvous phase, when the target is too small in the field of view for geometry tracking to be effective. Bearing is calculated by scanning the field of view and calculating the centroid of the valid data relative to the sensor. By measuring the motion of the centroid over time, closing rates can be estimated. For TriDAR, this state uses the on-board thermal imager for very long-range operations (tens of kilometers) and the 3D LIDAR for operations within ∼3 km.

The search mode calculates an initial guess of the target pose to initialize tracking. The initial guess can be obtained from external systems (e.g., GPS, inertial sensors, radar), from ground uplink, or via the use of internal automatic acquisition algorithms (Ruel, Luu, et al., 2008; Ruel, Ouellet, et al., 2008). The search can be constrained or unconstrained depending on the specific mission scenario, with processing time varying accordingly. If an approach corridor is specified, the search process will validate its estimate before allowing the system to proceed to the tracking state.

Once the target is localized, tracking is initiated. The sensor is then commanded to acquire 3D sparse data from areas of interest on the target. These scan areas typically change depending on the range to the target and the current point of view. These mission elements, as well as algorithm settings and target reference models, are specified in a mission configuration database used by the onboard software. The software then uses the algorithms presented in the previous sections to perform pose estimation and update the current state vector.

4. TRIDAR SENSOR HARDWARE

The TriDAR 3D Sensor hardware was specifically designed to meet the needs of AR&D operations following the strategy presented in the previous sections. In particular, the sensor was designed to achieve

- *High dynamic range* to obtain high-quality 3D data on both dark and shiny surfaces over a wide operating range.
- *Random access* to obtain well-distributed sparse data from areas of interest in the field of view.
- *High accuracy* that improves with decreasing range.
- *Lighting immunity*, allowing the system to operate under all lighting conditions encountered in orbit.

4.1. Design Approach

To achieve a wide operating range and provide random access, a flying-spot active-scanner configuration was selected for the TriDAR 3D sensor hardware. Because the laser source energy is focused into a single collimated beam, a very long range can be achieved (up to 3 km with the current hardware). A dual-axis scanner configuration allows the sensor to steer the emission and collection apertures in order to collect data in areas of interest within its field of view, and effectively achieves almost infinite zoom. The optical system was configured to use a bistatic triangulation baseline, which separates emission and collection apertures. This significantly improves the sensor's dynamic range. The disadvantage of this configuration is that it results in a relatively slow sensor (∼10K samples/s) that must collect each measurement individually. This is not a problem for this application, because AR&D operations occur very slowly in space and the MILD approach requires very few data. In fact, the current hardware acquires the data necessary for pose estimation in ∼100 ms. A much faster sensor would generate too many data, requiring significant data transfer overhead and long algorithm processing time. In the case of the TriDAR sensor design, speed was traded for long operating range with high dynamic range detection. The tracking algorithm presented in this paper executes in ∼90 ms on TriDAR's onboard computer. Tracking operations at 5 kHz are therefore achievable with this system.

4.2. 3D Sensor Design

The TriDAR active 3D sensor (Figure 5) is a hybrid scanner that combines autosynchronous laser triangulation technology (Blais, Beraldin, El-Hakim, & Godin, 2003) with time-of-flight (TOF) ranging (LIDAR) in a single set of scanning optics. The hardware uses ∼65 W of power when operating at full speed.

The laser triangulation subsystem is largely based on the laser camera system (LCS) used to inspect the Space Shuttle's thermal protection system prior to each reentry (Deslauriers, Showalter, Montpool, Taylor, & Christie,

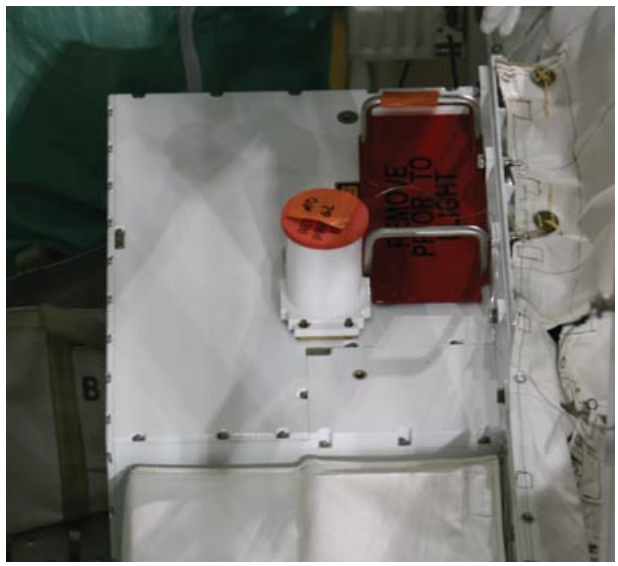

Figure 5. TriDAR flight hardware.

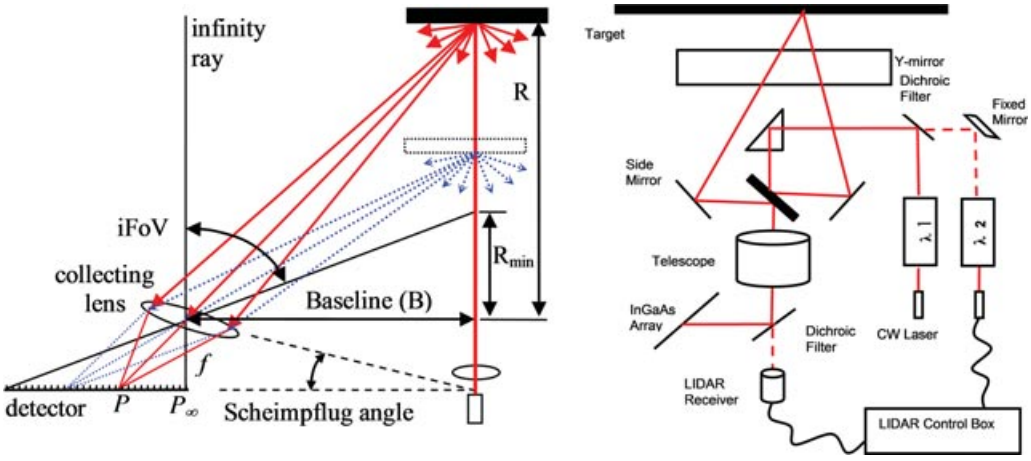

Figure 6. TriDAR triangulation geometry (left) and optical configuration (right).

2005). Figure 6 (left) shows the basic triangulation principle. A continuous-wave (CW) laser is projected onto a target surface. The location of the reflected image on an offset linear detector depends on the range to the surface at that projected location. Measurement of the image position then indicates range. The triangulation principle can provide very high-precision range measurements at close range, but the nature of the triangulation geometry means that imprecision grows approximately with the square of distance. Therefore, triangulation based systems tend to be practical only up to 10–20 m (Samson, English, Deslauriers, Christie, & Blais, 2002).

TOF LIDAR ranging uses a short laser pulse, a detector to measure the reflected pulse, and timing circuitry to measure the time between pulse emission and detection directly. The greatest advantage of this pulsed approach is that it can operate at long range (a few kilometers) with relatively constant range accuracy as long as enough reflected light can be collected to make a measurement. The diameter of the launch beam and its divergence limit the achievable lateral resolution. Operation at short range is more challenging, because strong signals can saturate detection electronics and short round-trip durations need to be resolved.

The TriDAR optically multiplexes the triangulation and LIDAR emission and collection apertures using dichroic mirrors (Figure 6 (right)). This allows the emitting lasers (triangulation CW and pulsed TOF lasers) and detectors' fields of view (FOV) to be steered by a single pair of scanning mirrors. The triangulation subsystem is used to make high-accuracy 3D measurement at short range, where the LIDAR is not as accurate and is potentially saturated by strong returns. The LIDAR is then used for measurements beyond the useful range of the triangulation subsystem to provide 3D data of sufficient quality for AR&D operations. LIDAR data can also be used at short range to fill in invalid triangulation measurements or serve as verification. Because the detectors' instantaneous FOV steered by the mirrors are very small, the TriDAR is insensitive to lighting conditions. The TriDAR sensor can therefore operate from full sunlight to complete darkness.

This configuration takes advantage of the complementary nature of the two ranging technologies used to provide 3D data at both short and long range without compromising performance (English, Zhu, Smith, Ruel, & Christie, 2005). By combining the two ranging subsystems' optical paths, the TriDAR can provide the functionalities of two 3D sensors in a single package. Both triangulation and LIDAR ranging capabilities can be used during short-range operations (<20 m), thus providing an extra level of fault tolerance in the system for the last critical part of docking. The two ranging subsystems share the same control and processing electronics, thus providing further savings compared to using two separate sensors to cover the same operational range.

4.3. Implementing the More Information, Less Data Approach

Using the TriDAR hardware, the MILD strategy is implemented by having the output of the processing algorithms drive the 3D scanner to gather only the data necessary to compute the next set of information. Sparse data are acquired by the sensor in the area of interest using a combination of scan patterns available to the algorithm (Figure 7). These scan patterns have been designed to provide sparse data while accelerating and decelerating the scanning mirrors smoothly.

The Lissajous pattern (left) has high point density in the corners and low in the center, making it useful for monitoring transitions at the edges. The rosette pattern (center) has highest point density at the center and lowest at the periphery. This makes it ideal for high-resolution imaging of central features, although maintaining width and height in less important regions for alignment stability and

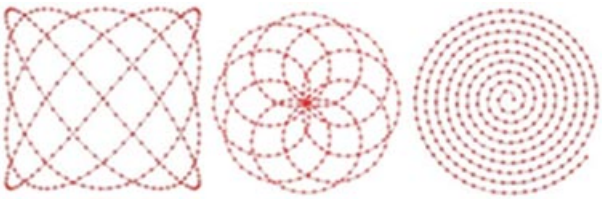

Figure 7. Typical TriDAR scan patterns.

monitoring purposes. The spiral pattern (right) is uniform in angular and radial spacing and hence ideal for surface digitization or inspection or for surfaces with uniform distribution of features. The phase of the waveforms can also be changed over time to increase the effective coverage of the target. Arbitrary patterns can also be used, limited only by the inertia of the scanning mirrors and power consumption budget. The three scan patterns in Figure 7 make optimal use of the natural sinusoidal inertias to cover an area in the shortest time with minimal power consumption.

5. STS-128 AND STS-131 TEST FLIGHTS

This section introduces the concept of operations for the TriDAR test flight onboard the Space Shuttle during rendezvous and departure operations to and from the ISS. Results from both missions are then presented.

5.1. Space Shuttle Rendezvous Operations

Space Shuttle rendezvous with the ISS typically occurs on flight day 3 (FD3) following a successful launch and orbit insertion. Phasing consists of a series of course correction burns that allow the shuttle to catch up with the ISS (Jang, 2001). Phasing burns are targeted in the Mission Control Center (MCC) using ground tracking. The exact timing of maneuvers varies depending on mission timeline and other constraints such as lighting.

Far rendezvous starts with a series of correcting combination (NCC) burns targeted onboard using relative navigation data aiming for a location ahead of and below the ISS, called the translation initiation point (Ti). Once the shuttle is at the Ti point, the new target point is the terminal phase point, which is located ~180 m below the ISS along the Earth radial axis, R-BAR (Figure 8). Before proximity operations are initiated, onboard navigation sensors include star trackers, GPS, radar, and an optical telescope called the crew optical alignment sight (COAS). TriDAR is nominally planned for activation during far rendezvous. Proximity operations start in the final phase of the rendezvous. During this phase, a pilot directly controls the orbiter along its translational axes while approaching the ISS.

At the terminal phase point, the shuttle commander controls the orbiter into a back flip maneuver called the R-BAR pitch maneuver (RPM). This maneuver is performed to allow the crew of the ISS to photograph the thermal protection system of the Space Shuttle for inspection purposes.

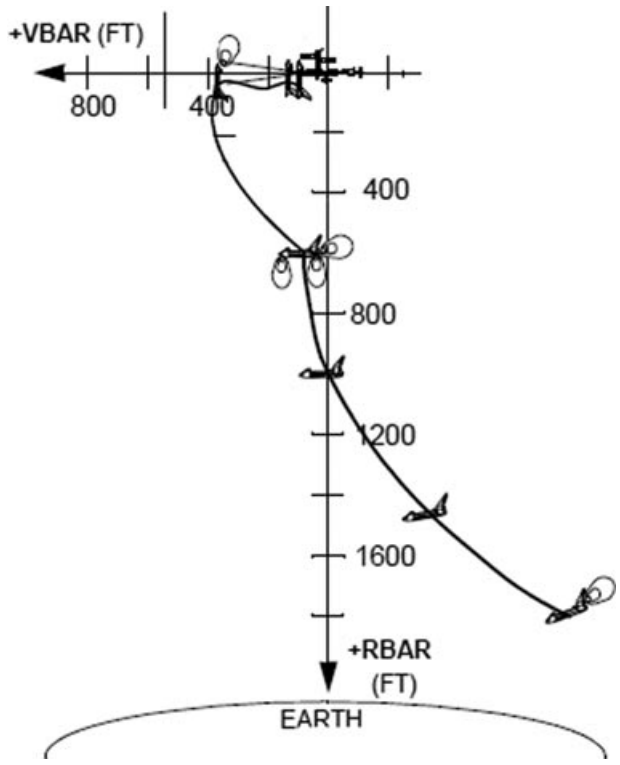

Figure 8. Space Shuttle proximity operations: nominal approach.

This maneuver constrains the laser power emitted by the TriDAR, as the ISS crew members are using high-powered optics to view and photograph the shuttle while the TriDAR is emitting laser energy at the ISS.

With the ISS almost in its final configuration, the Space Shuttle typically docks to the ISS at pressurized mating adapter (PMA) #2, located at the end of the ISS assembly pointing along the orbital velocity axis (+V-BAR). After the RPM, the shuttle is positioned ~180m below the ISS along the R-BAR and initiates a fly-around maneuver (TORVA) that will bring it in front of the ISS along the +V-BAR (Figure 8). The pilot then uses braking burns to maneuver the orbiter to a soft dock along the V-BAR axis. Navigation sensors for proximity operations may include the COAS, rendezvous radar, handheld LIDAR (HHL), and the trajectory control system (TCS). The HHL is aimed through the orbiter's overhead windows and triggered manually by crew members. The TCS system tracks retro-reflectors one at a time on the ISS to provide range, bearing, and rates to a specific point on the ISS.

5.2. Space Shuttle Undock and Fly-Around Operations

Separation from the ISS is initiated by releasing attaching hooks. Once the hooks are clear, springs push the interfaces

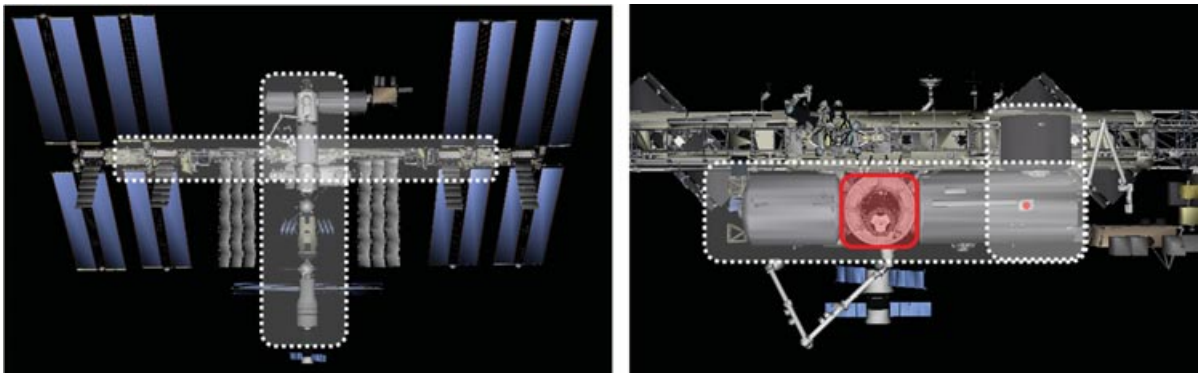

Figure 9. TriDAR tracking algorithm sensor scan targets for long-range approach (left) and short-range approach (right).

apart, providing the orbiter with enough opening rate to clear the docking port and initiate separation burn(s). The orbiter then proceeds along the V-BAR axis up to a distance of approximately 140 m. At this point, a fly-around maneuver is initiated. If enough propellant is available, the shuttle continues into a full fly-around at a nominal distance of 200 m before performing a separation burn that will initiate the return to Earth (refer to Figure 18 for the nominal profile). If propellant is not available, the orbiter can skip the fly-around and perform the separation burn directly. Once the separation burn has been performed, TriDAR loses sight of the ISS and is powered down by the crew.

5.3. Tracking Configuration for Operations to ISS

For missions to the ISS, the TriDAR mission configuration database (Section 3.3) was set up to support two different operations: docking and undocking. The primary difference between the two operations is that one is constrained to a certain approach corridor (R-BAR/V-BAR approach), whereas the other is unconstrained because of the fly-around. The drawback of unconstrained operations is primarily related to the processing time of the automatic target acquisition (ATA) algorithm. ATA for the docking operation usually occurs in under a second, whereas undock ATAs typically require 5–10 s on TriDAR's embedded flight computer.

The reference models used to provide the target geometry for the tracking algorithm were obtained from NASA. All Because the positions of moving elements such as solar panels, radiators, and robotic systems of the ISS at the time of rendezvous were not known, they were removed from the reference model to ensure that they would not be used by the algorithm. Any data obtained from these surfaces during the mission will be rejected as outliers by the algorithm and do not affect the solution.

Because of the size of the target, different tracking strategies are used throughout the rendezvous/departure operations. Strategies are selected based on range to the target and point of view. The system automatically switches strategy depending on the last known pose of the ISS and its trajectory. Transitions between triangulation and 3D TOF measurements are also performed automatically. For the TriDAR DTO missions, the transition to triangulation data occurred at ∼7 m from the docking port interface. Inside this range, TriDAR relied on the more accurate triangulation data, but still used less accurate LIDAR data to replace outliers and fill holes in the triangulation data.

Long-range operations primarily focused on tracking the cross formed by the ISS truss segments and the main ISS stack structure (Figure 9(left)). After the transition maneuver to the V-BAR approach (TORVA), the system aims for the docking area of the ISS, including the Japanese KIBO laboratory, the European Laboratory Columbus, the Pressurized Mating Adapter 2, and the ISS Node 2 (Figure 9 (right, dotted boxes)). Short-range operations focused on the geometry of the docking port itself (Figure 9 (right, solid box)). Tracking the docking interface geometry at close range is important because it minimizes any tracking error arising from flex distortions in the ISS structure compared to the ideal CAD models.

5.3.1. Mission Configuration Validation

To verify that algorithm settings will meet the specified performance for the approach corridor, including failure modes, an extensive simulation framework was developed. Because of the relative motion profiles, operating ranges, and sizes of targets in AR&D missions, it is impossible to fully test the system on the ground. Validation of the flight configuration database for both DTO missions involved extensive simulation testing with ground validation using half-scale models of the ISS at Neptec's Vision System Certification Laboratory (VSCL). Because of the criticality of the simulation testing for rendezvous sensors, a great deal of effort was dedicated to making the TriDAR simulator as realistic as possible.

The simulator developed for TriDAR emulates not only the imaging process of the sensor but all of the

software interfaces as well. In fact, the simulator uses a large portion of the actual TriDAR software. Only the low-level hardware interfaces are redirected to an emulation layer. This allows the simulator to be used with hardware in the loop, with the algorithms actually executing on the embedded flight processor. This configuration can even be used while integrated on the spacecraft. The simulator provides the capability to trigger failure modes in the system and test recovery routines. An interface is also provided to allow integration with guidance and navigation simulators in order to verify closed loop functionality and test the behavior of digital autopilot systems in response to the noise characteristics of the TriDAR. This capability was used to integrate the TriDAR simulator at Johnson Space Center's rendezvous simulation facility to facilitate crew training and interface verification.

Simulated data are very useful, because large datasets with known true pose can be obtained, and thus reliable statistics can be generated quickly. The problem commonly observed when data are simulated for active sensors is the poor realism of the sensor imaging model. Active sensors have biased noise and present distortions that are dependent on not only the sensor itself but also on the target being scanned. These effects must be taken into account for the data to be representative of what would be obtained from a real sensor. Neptec's sensor simulation framework takes into account the various parameters that affect a scan, such as range noise, laser source divergence, and pointing resolution, as well as interactions with target surface shape and materials. Different models are used internally to emulate data from the triangulation and TOF subsystems.

5.4. TriDAR Mission Overview

TriDAR was first tested in space on board Space Shuttle Discovery during the STS-128 mission to the ISS. The objective of this first test flight was to demonstrate the capability of the system to autonomously acquire and track the ISS without using retro-reflectors or other cooperative targets. To reproduce the conditions of an unmanned docking, the system was configured to perform the entire mission autonomously, automatically acquiring the ISS and producing 6 DOF state vectors in real time. The system was designed to self-monitor its tracking solution and was capable of automatically reacquiring the ISS if tracking was lost. The flight hardware (Figure 5) also included a thermal imager meant to extend the range of the TriDAR rendezvous sensor beyond the operating range of the 3D subsystem. The thermal imager was operated independent of the tracking capability for the first two demonstration missions. The camera was configured to perform self-calibration in orbit and automatically acquire data from ISS for postflight ground analysis that will serve as an input to the ongoing tracking algorithm development.

TriDAR was installed in the Space Shuttle's payload bay on the orbiter docking system (ODS) next to the TCS rendezvous sensor (Figure 10).

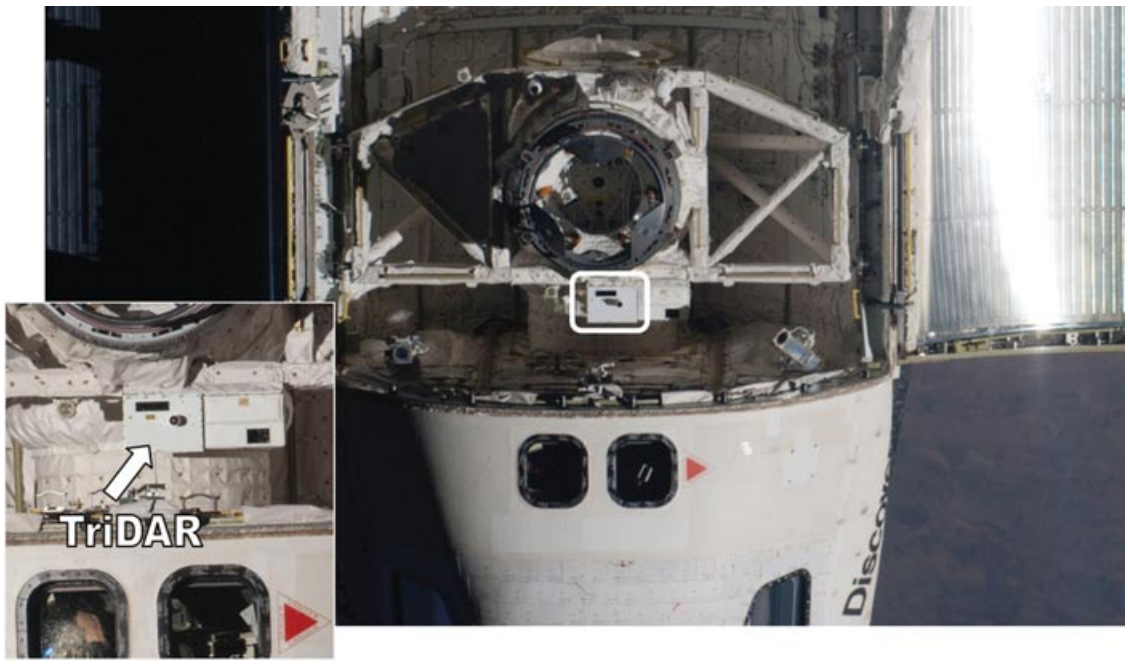

Figure 10. TriDAR flight unit installed in Space Shuttle Discovery's payload bay (STS-128). Photo courtesy of NASA.

The sensor was connected to a laptop computer inside Discovery's crew cabin. The laptop was used to command the system, log the data, and display the tracking solution and other system statuses to the crew in real time. All 3D data processing and state vector calculations were performed locally on the sensor in real time.

The specific configuration of the TriDAR laser hardware (Figure 5) used for these Space Shuttle missions was selected to meet NASA eye safety requirements and ensure safe operations for both shuttle and station crews. The ISS crew performs inspection of the Space Shuttle heat shield during the RPM maneuver shortly before docking (Section 5.1). This inspection is performed using high-magnification 20 × 60 binoculars and reflex cameras with telephoto lenses. This imposes serious limitations on laser-based systems to ensure the safety of both crews. For TriDAR, this resulted in a system configured with less than 10% of the laser power nominally available in the system, thus significantly reducing the operational range of the system to be flight-tested. This configuration was nevertheless sufficient to achieve mission objectives and demonstrate targetless tracking in orbit.

The missions involved TriDAR operations during both the docking and undocking/fly-around phases. This allowed two separate data collection opportunities. For docking operations, the system was activated during the final rendezvous course corrections (Section 5.1). After initialization, TriDAR entered a search mode where 3D and thermal imager data were acquired until a lock on a LIDAR signal was obtained. Once a signal was found, bearing and range information was provided until the target entered range for model-based tracking at approximately 200 m. Once in range, the system automatically acquired the ISS and allowed full 6 DOF tracking to start. Automatic tracking restarts were triggered every 5 min to exercise the ATA capability of the vision system at various points during the operation. For undocking and fly-around operations on STS-128, the system was configured in a data-gathering mode and continuously acquired 3D point clouds and thermal imager data. This mode was used to collect a rich dataset that can be used for future development of algorithms, as well as to protect against potential failures during real-time docking operations.

Building on the success of the STS-128 mission, the objective of the STS-131 TriDAR mission was to further test TriDAR AR&D sensor technology as it applies to satellite servicing. To meet the new objective, TriDAR was configured to autonomously track the ISS in real time during undocking and fly-around of the Space Shuttle. This provided a scenario similar to that of a tumbling target that would be encountered during servicing of a noncooperative spacecraft. New objectives also included longer-range acquisition from TriDAR's onboard thermal imager.

5.5. Rendezvous and Docking Operations

For both missions, TriDAR was activated during rendezvous operations on flight day 3. TriDAR's thermal imager detected the ISS at a range of 43.4 km, immediately after activation. The thermal imager detected the ISS under both day and night conditions and acquired over 3,000 high-quality images of the ISS during the rendezvous and docking operations. Figure 11 presents sample images at both long and short range, with color mapped to temperature.

TriDAR's TOF subsystem acquired the ISS at approximately 457 m. As mentioned previously, the TriDAR hardware allows a much larger operational range in its nominal configuration, but the performance of the flight-specific hardware was intentionally reduced to use less power and ensure eye safety of the ISS crew, who inspected the shuttle with high-powered optics during TriDAR operations. This

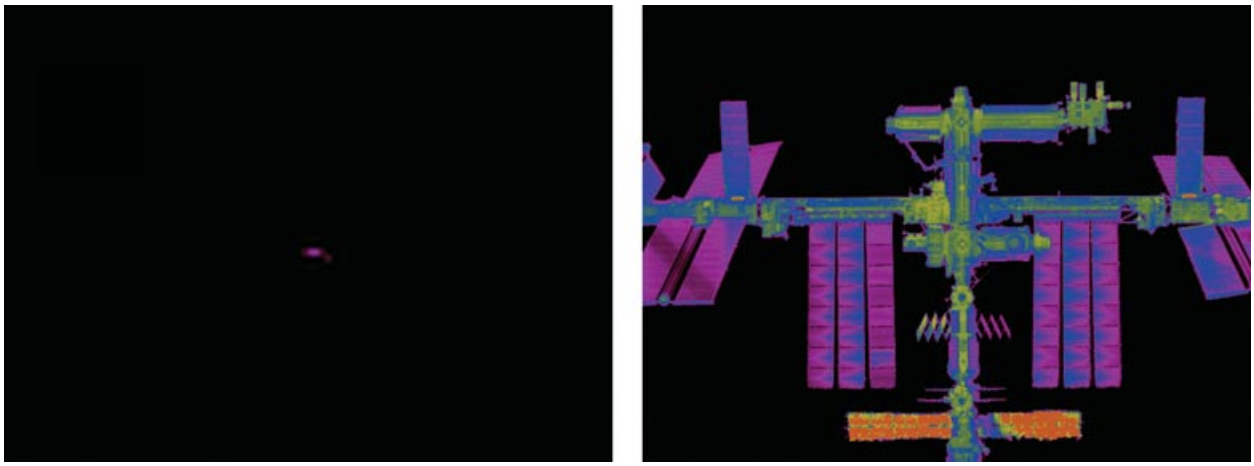

Figure 11. Thermal imagery of the ISS at 43 km (left) and 200 m (right).

design allowed mission objectives to be met despite ensuring crew safety. From initial acquisition onward, TriDAR provided the crew with bearing, range, and range rates to the ISS. No effects from ambient lighting conditions due to day/night transitions were observed during either mission.

TriDAR automatically acquired the ISS and successfully entered 6 DOF (relative position and attitude) tracking as the shuttle approached the ISS along the orbital velocity axis (V-BAR). Target acquisition and tracking were performed without the use of cooperative targets (visible, retro-reflector, or otherwise), and without any human intervention. TriDAR tracked the ISS in real time continuously up to docking, except for the planned 5-min automatic restarts, which were used to exercise the ATA capability. Tracking was successfully reestablished on all restarts without any human intervention. The tracking solution was displayed to the crew in real time (Figure 12) and matched the solution generated by the onboard shuttle rendezvous sensors within the limit to which they can be compared. Note that shuttle and ISS telemetry data were used to perform

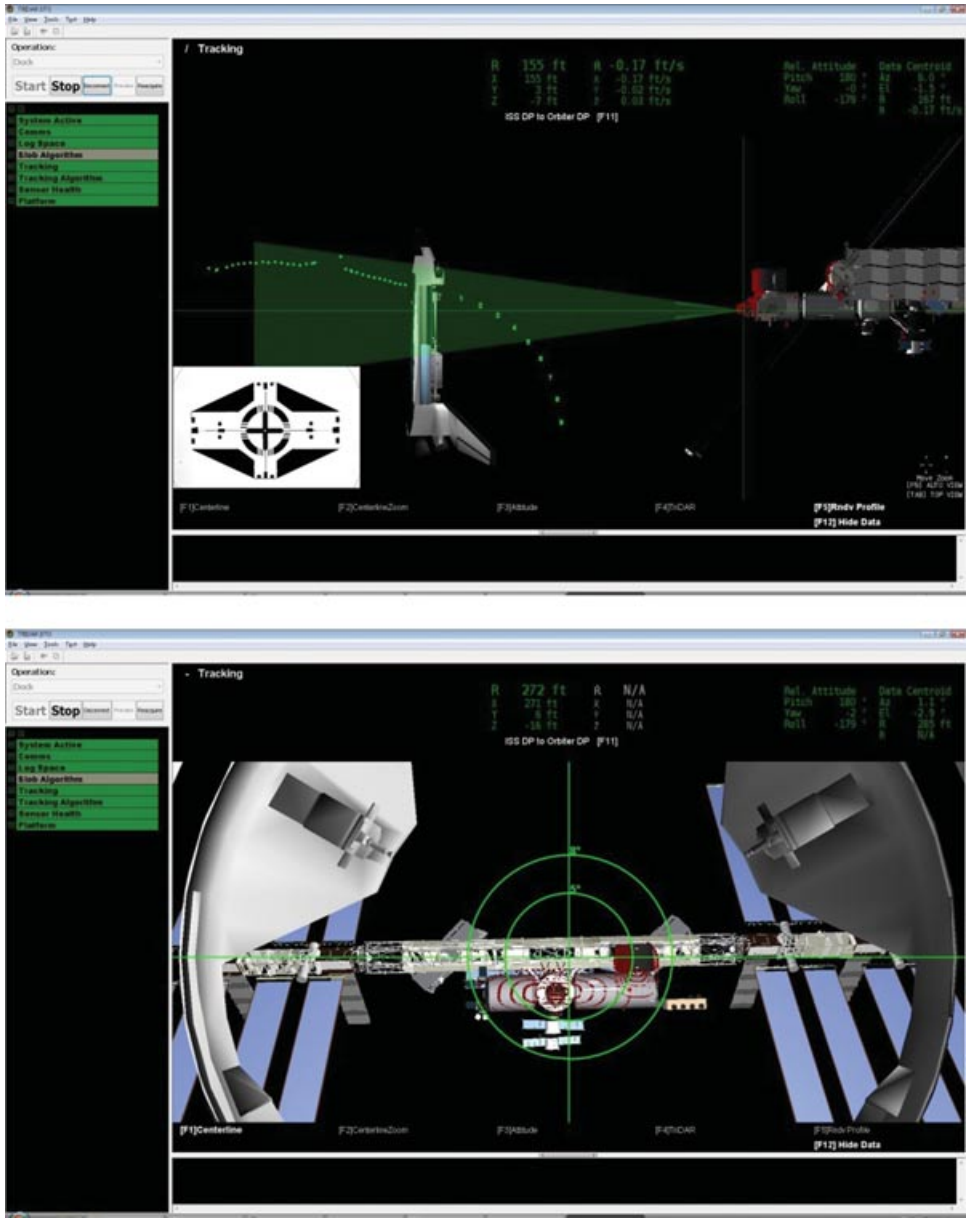

Figure 12. Real-time TriDAR crew displays. Trajectory view (left); centerline camera view (right).

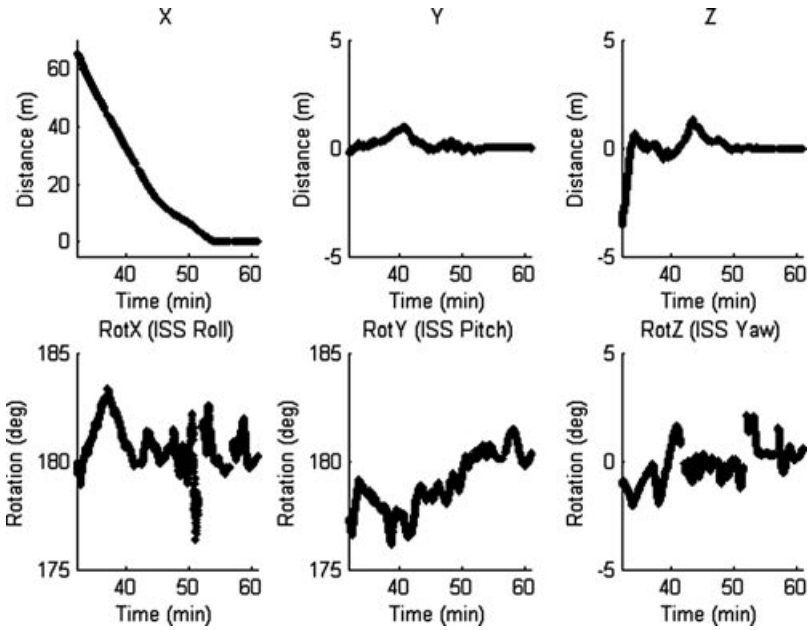

Figure 13. Relative pose of ISS with respect to orbiter.

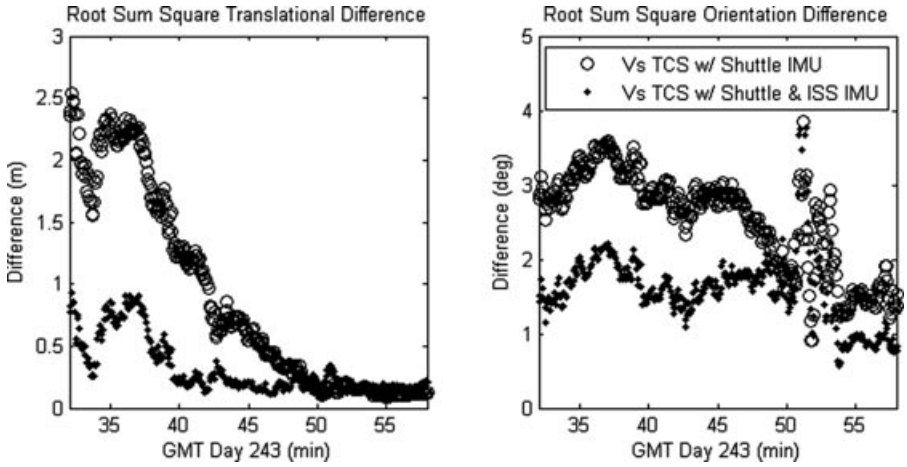

Figure 14. Difference between calculated TriDAR pose and shuttle onboard sensors.

comparisons, but the raw data are not presented in this paper, as they are proprietary to NASA.

Figure 13 presents the tracking solution of shuttle to ISS relative pose for the final portion of the docking as generated by TriDAR in real time during STS-128. Docking to the ISS on the STS-128 mission was performed without vernier jets on the orbiter, because of a failed thruster. This resulted in very active docking as can be seen in the plots. Note that the gaps in the data in Figure 13 correspond to the planned 5-min restarts of the system.

Figure 14 presents the root sum square of translational and rotational differences between the TriDAR and the sensors on board the shuttle. Note that these sensors have differing measurement characteristics with their own alignment and error budgets. None can be justified as a "true" reference from which quantitative performance metrics can be obtained. For example, combining the alignment and systematic error budgets for all the systems involved, quantitative comparisons can only be performed within a few degrees ($\sim 4^\circ$) (Jang, 2001). Furthermore, the onboard systems combine shuttle inertial sensors with the tracked 3D location of a known reflector on the station to calculate the relative position and orientation of the ISS. These systems do not take into account the actual real-time ISS

attitude, and assume it is holding in a known attitude. Because TriDAR provides a direct measurement of the position and orientation of the ISS relative to the shuttle, the sensor outputs line up more closely when factoring in the actual ISS attitude over time obtained from ISS IMU measurements (Figure 14). In the earlier part of the shuttle approach during STS-128, the ISS was flying a pitch attitude slightly different from that assumed by the onboard system (>1.2°). A ground call was made to the crew conveying this information. As the shuttle flew closer to the ISS, the ISS attitude was corrected to the expected attitude. The two curves in Figure 14 confirm this trend and, slightly before docking, all sensors converge to similar solutions. The TriDAR and shuttle sensors have a translational bias left because of an ∼0.1-m difference in their definition of the docked location along the docking axis. A rotation bias remains between the TriDAR and the shuttle onboard sensors, and this is found along the ISS pitch axis (rotation about the ISS main truss). It is believed that this bias is caused by flex in the ISS structure, which is currently being compensated for in the TCS system but not in the TriDAR. The transition from LIDAR data to triangulation data occurred when the shuttle was ∼7 m away from the ISS. The algorithm took longer than expected to converge on the triangulation data, which caused the noisy rotation pose measurements that can be observed at ∼52 min. This issue has been addressed in the system by changing the tracking algorithm settings when triangulation data are used.

Closing rates calculated by TriDAR matched with the shuttle TCS sensor very closely. The HHL is operated manually by crew members inside the crew cabin and provides a less reliable measurement, as can be observed in Figure 15. Note that, for the most part, the larger differences observed between the TCS and the TriDAR are primarily due to differences in how rates are calculated internally. TriDAR's rate calculation filter lags the TCS filter, which artificially introduces short-term differences when closing rates are changed because of shuttle maneuvers.

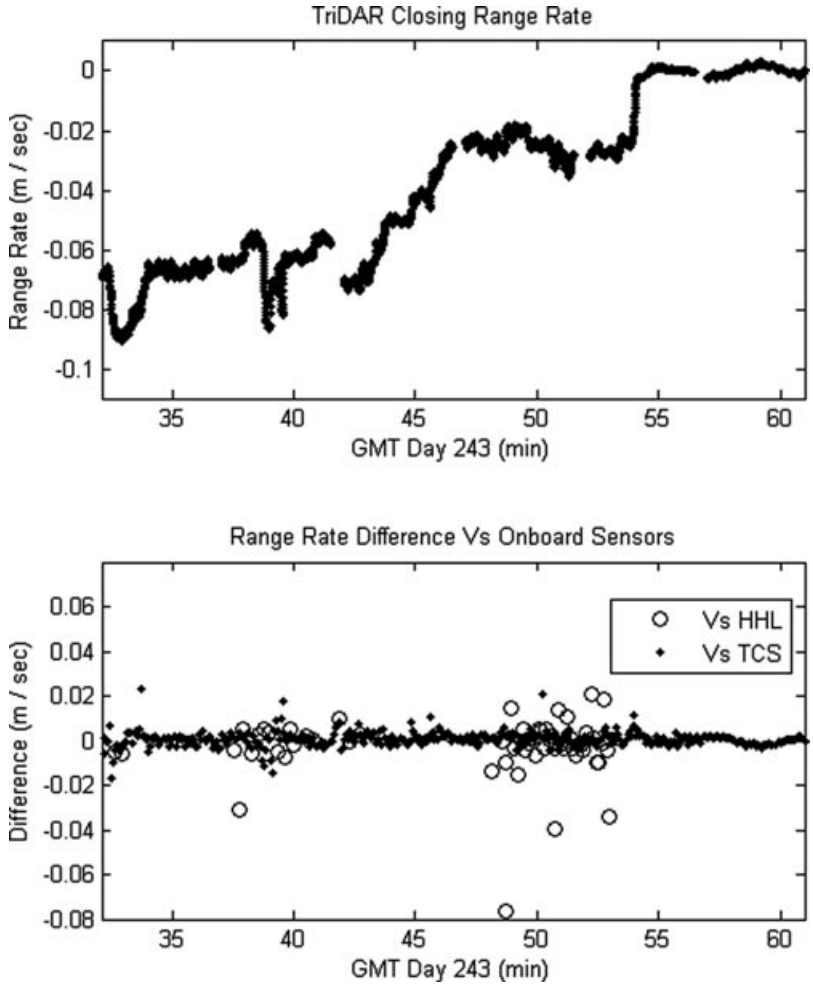

Figure 15. Closing rate as calculated by TriDAR (top) and difference in closing rate compared to shuttle onboard sensors.

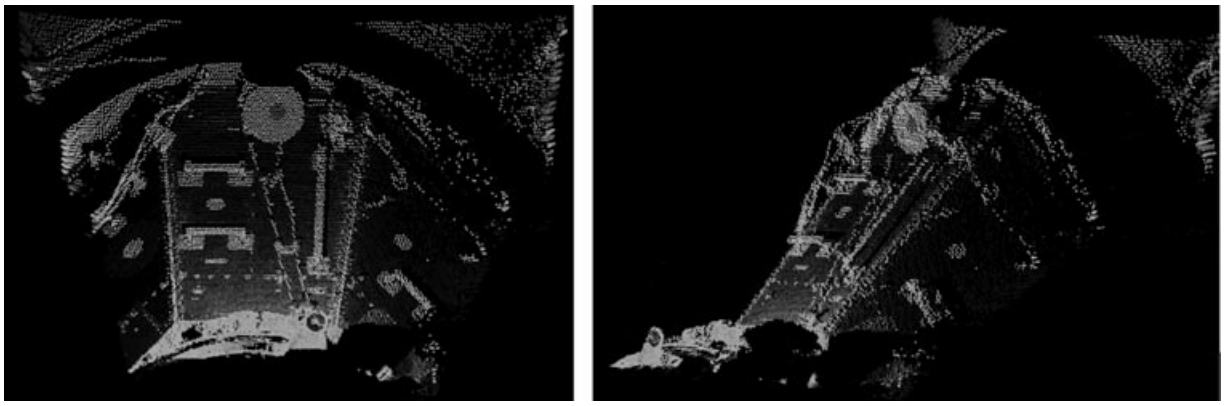

Figure 16. STS-128 postdock TriDAR inspection 3D scans.

5.6. Inspection Capability

After the orbiter docked to the ISS, the TriDAR acquired high-resolution 3D raster scans to demonstrate its inspection capability using high-accuracy triangulation data. Scans were acquired under day and night conditions, demonstrating the TriDAR's lighting immunity. Figure 16 shows raw triangulation data from PMA#2 obtained at the docking position.

5.7. Undocking and Fly-Around Operations

5.7.1. STS-128 Undock and Fly-Around

On its first flight, STS-128, TriDAR operated in data-gathering mode during undocking and fly around operations. In the course of departure from the ISS, the sensor acquired over 1,200 3D point clouds and IR images. The TriDAR showed excellent 3D data quality and return signal strength. 3D point cloud data showed no change in data quality from day/night transitions. Figure 17 presents color-coded 3D data obtained during undock and fly-around. The returns obtained from dark (PMA) and shiny surfaces (metal), as well as the returns from solar panels at high incidence angles, demonstrate the wide dynamic range achieved with the TriDAR sensor design.

The tracking algorithm was also applied off line to the data acquired during STS-128 undock and fly-around to generate the tracking solution that would have been obtained during flight. Using the same tracking algorithm used for flight, the system automatically acquired and tracked the ISS, calculating the relative pose for the entire 360° change in relative orientation. The calculated pose matched very well with the shuttle's onboard navigation system. Figure 18 (left) presents the calculated pose from flight data compared to the nominal rendezvous profile. Note that the fly-around was entered differently than planned, likely to save fuel. Also note that the ISS started maneuvering slightly after the shuttle undocked, which caused distortions in the plotted path.

5.7.2. STS-131 Undock and Fly-Around

Undock and fly-around tracking were performed in real time on STS-131. TriDAR automatically acquired the ISS

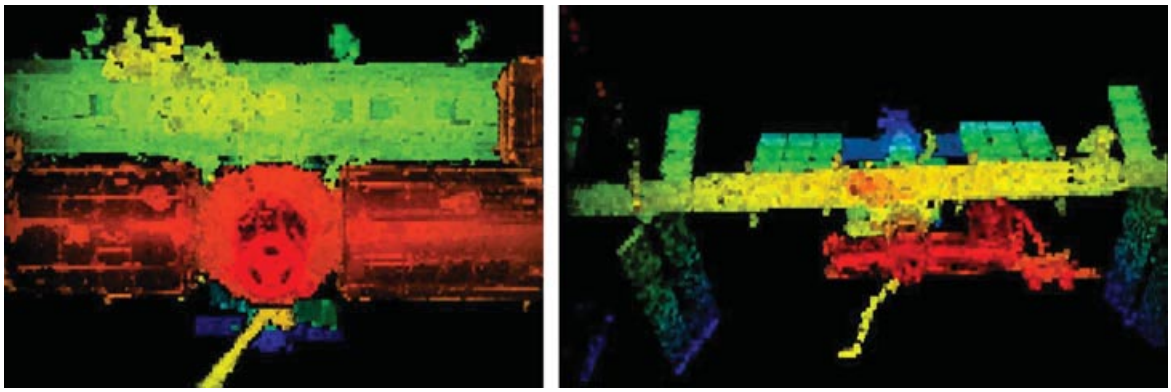

Figure 17. TriDAR 3D data acquired during STS-128 undock and fly-around operations.

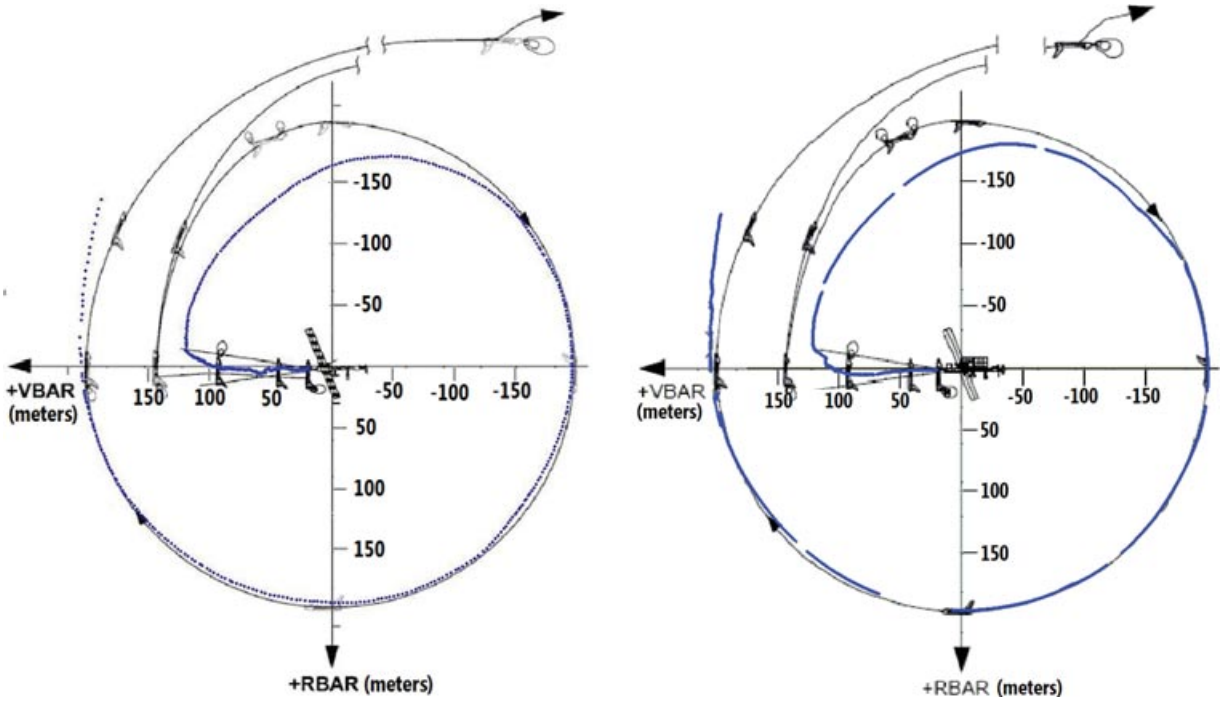

Figure 18. Shuttle fly-around trajectory (dotted line) as measured by TriDAR compared with baseline trajectory (black line) for STS-128 (left) and STS-131(right).

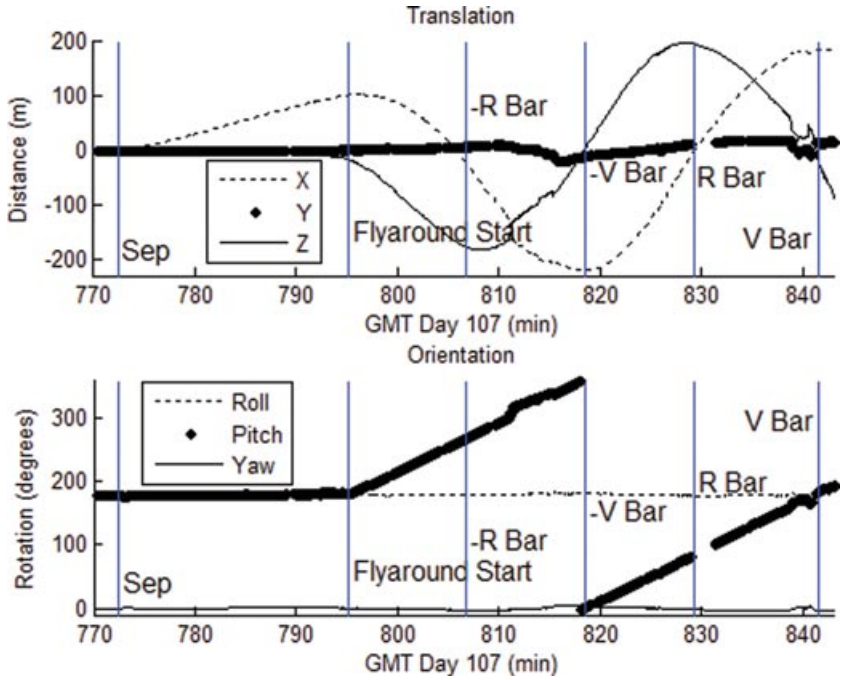

Figure 19. STS-131 shuttle fly-around state vector as calculated by TriDAR in real time.

and successfully performed 6 DOF position and orientation tracking upon activation prior to undock. TriDAR tracked the ISS continuously from pushback to the separation burn, when the ISS left the sensor's field of view. Similarly to the rendezvous and docking operations, TriDAR initiated planned 5-min automatic restarts to demonstrate ATA. In line with rendezvous and docking performance, tracking was successfully reestablished on all restarts without human intervention. Figure 18 (right) shows the tracking solution generated by TriDAR in real time during STS-131 plotted against the planned trajectory. Figure 19 shows the corresponding translation and rotation state vectors. Real-time operations during fly-around on STS-131 demonstrated TriDAR's ability to track a noncooperative, tumbling target, thus meeting the primary objective of the mission.

6. CONCLUSION

Neptec's TriDAR proximity operations vision system provides full 6 DOF relative state vectors for AR&D operations in space without requiring the use of cooperative targets. TriDAR uses knowledge about the shape of the target spacecraft, along with successive 3D point clouds acquired from a hybrid 3D scanner, to automatically acquire and track an object in real time.

The vision system was selected for test flights on board Space Shuttle Discovery during the STS-128 and STS-131 missions to the ISS. The objective of the missions was to demonstrate TriDAR's automatic targetless tracking ability during ISS rendezvous, docking, undocking, and fly-around operations. During both test flights, TriDAR successfully acquired and tracked the ISS in real time, providing state vectors and closing rate information to the Space Shuttle crew. During STS-131, TriDAR autonomously acquired and tracked the ISS in real time for the entire 360° fly-around. This demonstrated TriDAR's ability to track tumbling, noncooperative targets, which is an important capability for satellite servicing applications. TriDAR met all primary mission objectives for these initial test flights. Although TriDAR was developed primarily for unmanned missions, the system proved useful for manned operations as well, because it provides another input for pilots to cross check information from other sensors. The initial flights of TriDAR marked a first in space for noncooperative 3D-based rendezvous and docking proximity operation vision systems. TriDAR is scheduled to fly on a third test flight on board the Space Shuttle during the STS-135 mission to the ISS. This mission will test improved hardware and a real-time thermal imager tracking capability that was developed based on data obtained from the first two missions.

With the retirement of the Space Shuttle, several new vehicles will be used to resupply the International Space Station (ISS). These include Orbital Sciences Cygnus, SpaceX's Dragon, the European Transfer Vehicle (ATV), and the Japanese H-II Transfer Vehicle. With demonstrated ISS rendezvous and docking capability, TriDAR can easily be adapted to operate on any of these vehicles. Because TriDAR does not rely on cooperative targets on the ISS, it brings flexibility in the choice of docking location and approach trajectory. The geometry-tracking capability of TriDAR could also be used to monitor and track visiting vehicles from the ISS independently without having to modify each vehicle to add reflectors.

7. APPENDIX: INDEX TO MULTIMEDIA EXTENSIONS

The videos are available as Supporting Information in the online version of this article.

Extension	Media type	Description
1	Video	*STS-128 Docking Replay.wmv*: Replay of the final portion of rendezvous and docking operation during the STS-128 mission using tracking data generated by TriDAR as seen from the docking port's centerline camera point of view. Actual video from the centerline camera is overlaid (top right corner), showing the "as observed" relative pose. A red X appears when the system is performing a planned reacquisition every 5 min, indicating that no tracking data are available during this time. Note that the video is sped up ∼20 times.
2	Video	*STS-128 Flyaround 3D Pointcloud Data.avi*: Presents all of the raw 3D data acquired by the TriDAR sensor during STS-131 undocking and fly-around. The data are color coded as a function of range.
3	Video	*STS-131 Docking IR Camera.wmv*: Presents raw thermal imager data acquired during rendezvous operations on STS-131. The plot on the right indicates where the shuttle was in its approach and what its attitude was. Day/night conditions are also displayed.
4	Video	*STS-131 Undocking Tracking Replay.wmv*: Replay of the STS-131 undocking and fly-around operation using tracking data generated by TriDAR in real time. Red dots are raw sensor 3D measurements used to generate the tracking data. Video is sped up.

REFERENCES

Besl, P. J., & McKay, N. D. (1992). A method for registration of 3-D shapes. IEEE Transactions on Pattern Analysis and Machine Intelligence, 14(2), 239–256.

Blais, F., Beraldin, J.-A., El-Hakim, S., & Godin, G. (2003, Sept. 22–26). New development in 3D laser scanners: From static to dynamic multi-modal systems. Proceedings of 6th Conference on Optical 3D Measurement Techniques, Zurich.

Chen, Y., & Medioni, G. (1992). Object modeling by registration of multiple range images. Image and Vision Computing, 10(3), 45–155.

Creamer, G. (2007). The SUMO/FREND Project: Technology development for autonomous grapple of geosynchronous satellites. Advances in the Astronautical Sciences, 128, 895–910.

Deslauriers, A., Showalter, I., Montpool, A., Taylor, R., & Christie, I. (2005, April). Shuttle TPS inspection using triangulation scanning technology. Paper present at SPIE 2005, Orlando, FL.

English, C., Okouneva, G., Saint-Cyr, P., Choudhuri, A., & Luu, T. (2011). Real-time dynamic pose estimation systems in space: Lessons learned for system design and performance evaluation. In Special issue on "Quantifying the performance of intelligent systems," International Journal of Intelligent Control and Systems, 16(2), 79–96.

English, C., Ruel, S., Melo, L., Church, P., & Maheux, J. (2004, April). Development of a practical 3D automatic target recognition and pose estimation algorithm. In SPIE Defense & Security Symposium Proceedings on Automatic Target Recognition XIV, Orlando, FL (Vol. 5426, pp. 102–111).

English, C., Zhu, X., Smith, C., Ruel, S., & Christie, I. (2005, September). TriDAR: A hybrid sensor for exploiting the complementary nature of triangulation and LIDAR technologies. In Proceedings of the ISAIRAS 2005 Conference (ESA SP-603), Munich, Germany.

ESA. (2008). Rendezvous and docking technology (ATV Information Kit). Noordwijk: ESA.

ESA Media Relations Office. (2008, April). Europe's automated ship docks to the ISS. European Space Agency news. Noordwijk: ESA

Fehse, W. (2003). Automated rendezvous and docking of spacecraft. Cambridge Aerospace Series (No. 16). Cambridge, UK: Cambridge University Press.

Howard, R. T., Heaton, A., Pinson, R., Carrington, C., Lee, J., Bryan, T., Robertson, B., Spenser, S., & Johnson, J. (2008, March). Orbital express advanced video guidance sensor. Paper presented at the 2008 IEEE Aerospace Conference, Big Sky, MT.

Jang, P. H. (2001). Rendezvous and proximity operations design reference for the international space station, Revision D (JSC-27240). Houston: NASA JSC.

MacLean, S., & Pinkney, L. (1993). Machine vision in space. Canadian Aeronautics and Space Journal, 39(2): 63–77.

Mokuno, M., Kawano, I., & Kasai, T. (1999, February). Experimental results of autonomous rendezvous docking on Japanese ETS-VII satellite. In Proceedings of 22nd Annual AAS Guidance and Control Conference (AAS-99-022), Breckenridge, CO.

Mokuno, M., Kawano, I., & Suzuki, T. (2004). In-orbit demonstration of rendezvous laser radar for unmanned autonomous rendezvous docking. IEEE Transactions on Aerospace and Electronic Systems, 40(2), 617–626.

Obermark, J., Creamer, G., Kelm, B., Wagner, W., & Henshaw, C. (2007). SUMO/FREND: Vision system for autonomous satellite grapple. Proceedings of the SPIE, 6555, 65550Y.

Polites, M. M. (1998, July). An assessment of the technology of automated rendezvous and capture in space (NASA/TP-1998-208528).

Ruel, S., English, C., Anctil, M., & Church, P., (2005, September). ^{3D}LASSO: Real-time pose estimation from 3D data for autonomous satellite servicing. In Proceedings of the ISAIRAS 2005 Conference (ESA SP-603), Munich, Germany.

Ruel, S., English, C., Anctil, M., Daly, J., Smith, C., & Zhu, S. (2006). Real-time 3D vision solution for on-orbit autonomous rendezvous and docking. Proceedings of the SPIE, 6220, 622009.

Ruel, S., English, C., Melo, L., Berube, A., Aikman, D., Deslauriers, A., Church, P., & Maheux, J. (2004, April). Field testing of a 3D automatic target recognition and pose estimation algorithm. Presented at the SPIE Defense and Security Symposium, Orlando, FL.

Ruel, S., Luu, T., Anctil, M., & Gagnon, S. (2008, March). Target localization from 3D data for on-orbit autonomous rendezvous & docking. Presented at the IEEE Aerospace Conference, Big Sky, MT (pp. 1–11).

Ruel, S., Ouellet, D., Luu, T., & Laurendeau, D. (2008, February). Automatic tracking initialization from TriDAR data for autonomous rendezvous & docking. In Proceedings of the ISAIRAS 2008 conference, Hollywood, CA.

Rusinkiewicz, S., & Levoy, M. (2001, May–June). Efficient variants of the ICP algorithm. In Proceedings of 3DIM, Quebec City, Canada (pp 145–152).

Samson, C., English, C., Deslauriers, A., Christie, I., & Blais, F. (2002, April). Imaging and tracking elements of the International Space Station using a 3D autosynchronized scanner. In Proc SPIE AeroSense 2002, Orlando, FL, (Vol. 4714, pp. 87–96).